Spatiotemporal profiles of water quality at a new large tropical hydroelectric dam reservoir

[1]Teck Y. Ling, [1]Kong S. Phang, [2]Chen L. Soo, [1]Lee Nyanti, [1]Siong F. Sim, [1]Jongkar Grinang

[1] Faculty of Resource Science and Technology, Malaysia Sarawak University, Kota Samarahan, Sarawak, Malaysia; [2] Institute for Tropical Biology and Conservation, Malaysia Sabah University, Jalan UMS, Kota Kinabalu, Sabah, Malaysia. Corresponding author: T. Y. Ling, tyling@unimas.my

Abstract. The building of the Murum hydroelectric dam resulted in the formation of a reservoir in the year 2014. The newly formed reservoir can also serve as a cage aquaculture site in addition to fisheries. Therefore, it is important to determine the spatiotemporal profiles of water quality in the new reservoir and assess its suitability for fisheries and aquaculture. Water quality of riverine inflows and depth profiles of water quality in transitional and lacustrine zones were studied. Four samplings were conducted in 2017 at two stations each in the riverine and transitional zones, and three stations in the lacustrine zone. Results of the year-long study indicate that the riverine zone serves as the main input of suspended solids and organic matter to the reservoir which affected the pH and conductivity depth profiles particularly in the transitional zone due to anthropogenic activities in the river basin. Thermal stratification was apparent and consistent in the lacustrine zone throughout the year; whereas it was less consistent in the transitional zone and varied between stations receiving different riverine inflows at different times of the year. The colder sediment-laden inflows from the rivers influenced the depth profiles of the transitional and lacustrine zones especially after rainfall events. The DO values in transitional zone remained high due to the oxygenated riverine inflows. However, it dropped below the limit of 5 mg/L at the thermocline, and developed an anoxic condition at the deeper water column in the lacustrine zone throughout the year. A decrease in pH and an increase in conductivity, turbidity, TSS, CO_2, BOD_5, COD and TAN with depths were also observed in the lacustrine zone which are associated with the decomposition of organic matter and sedimentation. Since the depth of water column that contained healthy DO value of at least 5 mg/L for healthy life of aquatic organisms at the lacustrine zone was less than 1 m to 5 m coupled with the acidity of the water, it is not suitable for sensitive aquatic organism yet. At the riverine zone, even though DO is high, the high turbidity, TSS, and low pH render the water unsuitable for sensitive aquatic organisms. It is recommended that inputs of sediment and organic materials to the reservoir be reduced not only for the sustainability of the hydropower generation but also for fisheries and aquaculture development in the future.

Key Words: aquaculture, Murum dam, thermocline, oxycline, sedimentation, stratification.

Introduction. Even though dams are built across rivers to tap the hydropower from nature, the reservoirs formed could be sites for fish cage aquaculture (Costa-Pierce 1997) especially in developing countries like Malaysia (Abery et al 2005; Ling et al 2013; Ling et al 2018). However, the water quality of a reservoir has to be assessed for suitability for aquaculture development. In addition, good water quality is essential for reservoir fisheries as well. A number of factors potentially affect the water quality of a reservoir. Due to the accompanying infrastructure development and thus accessibility, land-based agriculture is developed and the extraction of timber continues in the river basin may continue both of which may impact the water quality of the new water body. The building of a dam itself alters the ecosystem from lotic to lentic typically resulting in a change in water quality (Ling et al 2017). In the reservoir, stratification pattern is a unique characteristic in reservoirs which plays a great role in several aspects of ecology (Agostinho et al 2008; Santos et al 2015). The thermal or chemical stratification appears in the water column soon after the reservoir is filled (Nyanti et al 2012; Ling et al 2016; Sapis et al 2017). This usually happens when the open surface water warms up and becomes less dense which renders it unable to mix with cold dense bottom water.

Subsequently, deterioration of environmental quality occurs including anoxic condition and acidification may occur in some layers of the water column due to the lack of water mixing (Elci 2008).

In temperate regions, the stratification in reservoirs are mainly related with seasons, whereas stratification structure of reservoirs in tropical regions tends to be associated with climatic events (Wang et al 2011; Jones et al 2011; Zhang et al 2015a,b; Zhou et al 2015). The river inflow has also been shown to influence the stratification structure of the reservoir (Laborde et al 2010; Araujo et al 2011). In general, a river inflow could enter a reservoir in several forms. The river inflow forms an underflow if the river water is denser than the reservoir water or an overflow if the river water is less dense than the reservoir water. The depth and the vertical extent of the intrusion are governed by density gradients and the mixing process. High volume of riverine inflows following rainfall and storm events also considerably influences the stratification patterns of the reservoir (Faithful & Griffiths 2000; Li et al 2015).

The large Murum dam in Sarawak was built across the Murum River located at the upper reach of Rajang River, right upstream of the Bakun dam in Sarawak, Malaysia. The filling of Murum began in September of 2013 and the first turbine discharge took place on November 2014. The river basin is subjected to active logging and plantation activities (Sapis et al 2018). Studies have shown that river water that flowed into the Bakun reservoir in the same region contained high turbidity and suspended solids (Ling et al 2015). The cold sediment-laden river inflows could form a density current and intrude the reservoir, influencing the depth profile of the reservoir. As the density gradients are constantly changing, the depth and vertical extent of the intrusion reached by the density current are more susceptible to change temporally. Knowledge of such changes is essential for future aquaculture development and fisheries industry. Hence, the objective of the present study was to assess the spatiotemporal depth profiles of the water quality at the new Murum reservoir.

Material and Method. The present study was conducted at the large Murum Hydroelectric Reservoir which is located at the north-eastern part of Sarawak, Malaysia (Figure 1). Two major rivers flowing into the reservoir are the Plieran River and the Danum River. The Murum reservoir was divided into three functional zones which are, riverine, transitional, and lacustrine zones. A total of seven sampling stations were selected in the present study. Two stations were located in the riverine zone of the reservoir where stations 1 and 2 were located at the Plieran River and Danum River, respectively. Station 3 and station 4 were located in the transitional zone receiving inflows from the Plieran River and Danum River, respectively. Three stations were located in the lacustrine zone of the reservoir where station 7 was the closest station to the dam.

Four samplings were conducted at intervals of three months in the year 2017. In-situ measurements including temperature, dissolved oxygen (DO), pH, conductivity, and turbidity were taken at all stations using a multiparameter water quality sonde (YSI 6920 V2-2). Flow velocity was measured using a stream flow meter (Geopacks) at stations 1 and 2 in riverine zone. The river width and depth were measured by using a range finder (Bushnell, Elite 1500) and a depth sounder (Hondex, PS-7 LCD), respectively. Total discharge, mean velocity, and mean depth were calculated according to Chapra (1997). At the riverine zone at stations 1 and 2 subsurface readings were taken whereas at stations 3 and 4 in transitional zone measurements were made from the surface down to the bottom of the water column. Depth profiles at stations 5, 6, and 7 in lacustrine zone were measured from the surface down to a depth of 50 m.

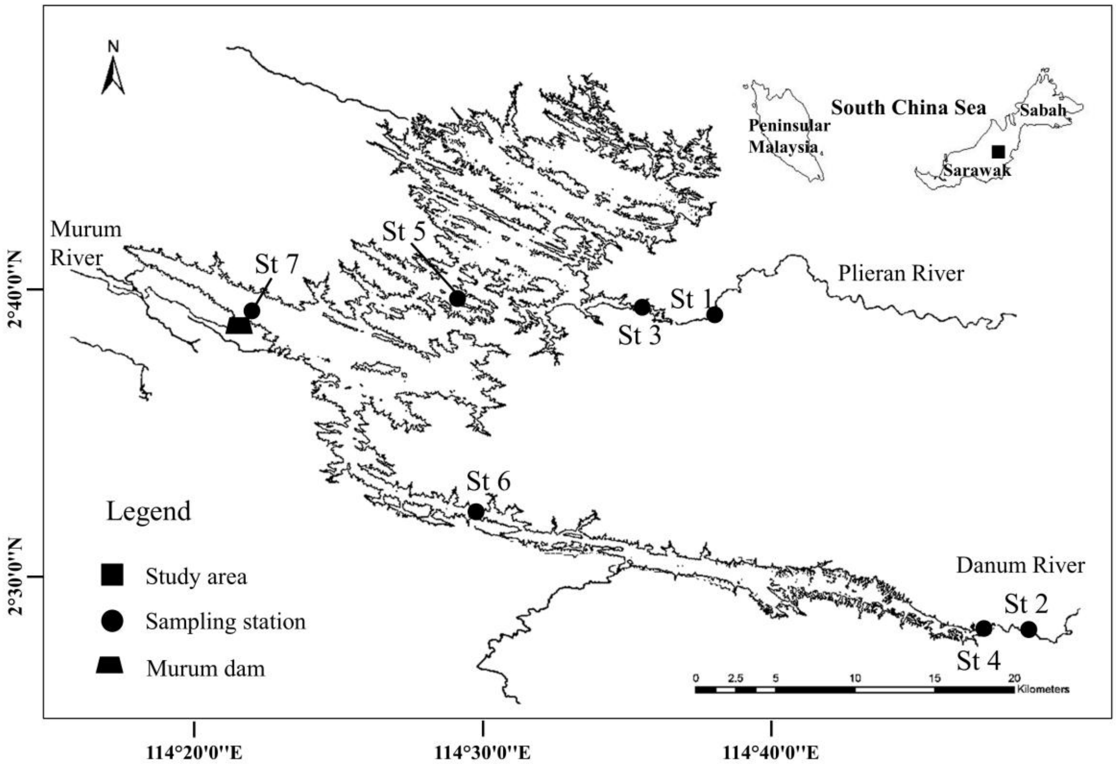

Figure 1. Location of the Murum reservoir in Sarawak state and the seven sampling stations in the reservoir.

Water samples were also collected in triplicates for ex-situ analysis using pre-washed polyethylene water bottles. The bottles were rinsed using water samples before filled with samples. At riverine zone (stations 1 and 2), subsurface water samples were collected. At transitional and lacustrine zones, the water samples were collected at 10 m depth interval whenever possible. The parameters analyzed included total suspended solids (TSS), biochemical oxygen demand (BOD_5), chemical oxygen demand (COD), free carbon dioxide (CO_2), and total ammonia nitrogen (TAN). TSS, BOD_5 and COD were analyzed according to Standard methods (APHA 2005). For TSS, Sartorius Stedim Biotech glass-microfibre disc filter papers, grade MGB of 1.0 µm retention with diameter of 47 mm, were used for this analysis. The filter papers prior to filtration and after filtration were dried in an oven at 105 °C until constant weight. The weight difference was used to calculate the concentration of TSS.

For BOD_5 analysis, when the sample pH was less than 6, the pH of water was adjusted by using 1 N NaOH until 7 followed by addition of dilution water in the ratio of 1:1. Then, seed suspension was added (1 mL of seed in 300 mL of sample). When DO of the sample was less than 5, the water was transferred into a container and shaken vigorously in order to aerate the water samples. The DO value stabilized after shaking was recorded as the initial DO. BOD bottle with the sample was wrapped with aluminum foil was incubated for five days before the final DO was taken. BOD_5 (mg/L) was calculated using the following formula:

$$BOD_5 = \frac{(D_1 - D_2) - (S)(Vs)}{P}$$

Where: D_1 is DO of diluted sample immediately after preparation, mg/L; D_2 is DO of diluted sample after the five days' incubation at 20 °C, mg/L; S is oxygen uptake of seed, Δ DO/mL seed suspension added per bottle (S = 0 when sample was not seeded); V_s is volume of seed in the respective test bottle, mL; P is decimal volumetric fraction of sample used.

COD was analyzed using the closed reflux, titrimetric method. A water sample of 2.5 mL was pipetted into culture tube. Then, 1.5 mL 0.01667*M* standard $K_2Cr_2O_7$ digestion solution and 3.5 mL H_2SO_4 reagents were added into the culture tube. The culture tube was capped tightly and inverted before being heated for 2 hours at 150°C by using a reactor (Hanna Instruments C 9800). After the digestion, the sample was cooled to room temperature and poured into a conical flask. Two drops of ferroin indicator were added. Then, the solution was titrated using 0.025 M standard ferrous ammonium titrant solution (FAS). The endpoint of the COD titration was observed when there is a sharp change of color, from the blue-green to light brown. COD concentration was calculated according to APHA (2005).

For TAN, the water sample (100 mL) was distilled using a semi-automatic Kjeldahl distillation unit (VELP Scientifica UDK 139) and the distillate was collected in 10 mL of boric acid (H_3BO_3). The distillate was collected and top up to 100 mL before analyzed using Nessler's method (HACH 2002). The absorbance was measured at the 425 nm wavelength by using a spectrophotometer (DR3900). TAN concentration was determined by using a calibration curve. As for quality control, two standards were tested with each set of samples and the analysis was repeated whenever the recovery percentage of known standards were not within the range of 90–100 %. CO_2 was analyzed according to the Method 8223 Buret titration (HACH 2002) where 100 mL of a water sample was titrated with 0.0227 *N* NaOH with phenolphthalein as an indicator.

One-way ANOVA was conducted to test significant difference in the ex-situ parameter means among the stations and among sampling depths and also among sampling trips. When there was significant difference, Tukey's test was used to do pair-wise comparisons. Bivariate correlation between the parameters at specific depths was conducted using SPSS 21.0.

Results and Discussion. Hydrogeometry data collected at the sampling stations in the riverine zone of the Murum reservoir are shown in Table 1. Data show that the river width, depth, velocity of water and the discharge were different among the months. Similarly, they differed between the two rivers with Plieran River showing higher discharge than Danum River due to higher velocity of flow most of the time and higher width.

Table 1

Hydrogeometry data of the sampling stations in the riverine zone of the Murum reservoir collected in 2017

Station	*Sampling trip*	*River width (m)*	*Mean depth (m)*	*Mean velocity ($m\ s^{-1}$)*	*Discharge ($m^3\ s^{-1}$)*	*Remarks*
1 Plieran	February	57.1	3.7	1.02	216.5	No rain a day before sampling
	May	84.7	7.2	1.09	661.5	Rained a day before sampling and raining during sampling
	August	79.3	4.6	1.80	658.6	Rained for nine days before sampling
	November	59.0	8.6	1.24	630.9	Rained a day before sampling
2 Danum	February	37.0	1.5	0.50	28.2	No rain a day before sampling
	May	36.0	5.3	1.23	234.6	Rained a day before sampling
	August	42.2	4.0	0.83	139.7	Rained for nine days before sampling
	November	33.7	3.5	0.35	42.1	Rained a day before sampling

In the riverine zone, the largest difference in water temperature spatially, namely between station 1 at Plieran River and station 2 at Danum River was 1.03°C which occurred in May. Other than that, the differences were small both spatially and temporally as illustrated in Figure 2.

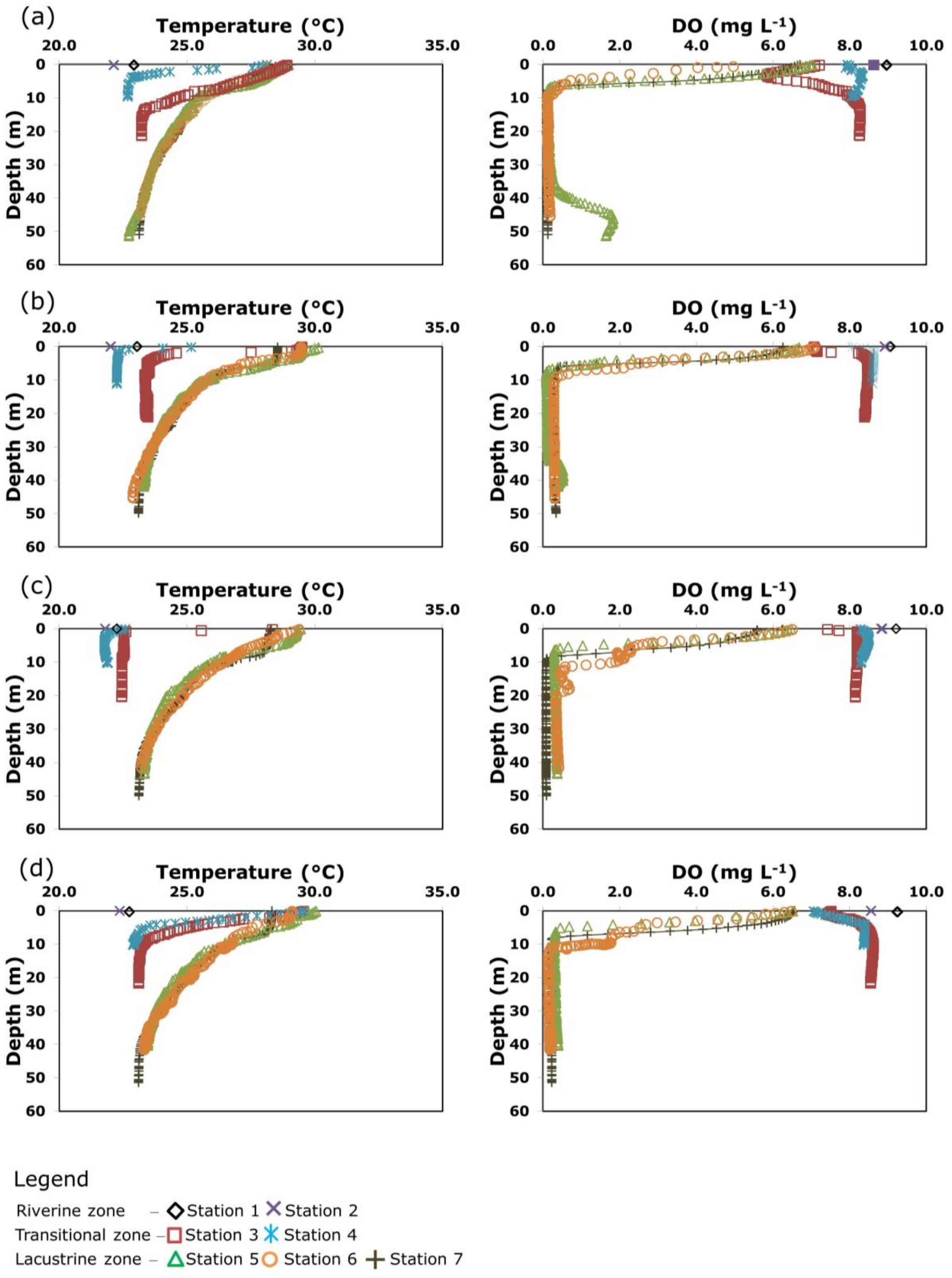

Figure 2. Depth profiles of temperature and DO measured in (a) February, (b) May, (c) August, and (d) November 2017 at the Murum reservoir.

The surface water is always the coolest (≈22.4°C) in the riverine zone due to the fast following water and the greater amount of canopy coverage. On the other hand, the open waters as in transitional and lacustrine zones have higher surface water temperature (>28°C) due to direct solar heating of the water body. Occasionally, low surface water temperature was observed at station 4 in the transitional zone. Vertical water temperature profile shows that water temperature decreased with depth in the transitional and lacustrine zones (Figure 2). The depth and strength of the thermocline varied spatially and temporally in the transitional zone of the reservoir. Station 3 that receives inflow from the Plieran River had thicker thermocline layer than station 4 that receives inflow from the Danum River. The depth of the thermocline at station 3 ranged from less than 1 m to 13 m whereas the depth of the thermocline at station 4 ranged from less than 1 m to 5 m. Thermocline layer of both stations were thicker in February and November than those in May and August. The main factors that affected the depth and thickness of the thermocline in the transitional zone include environmental conditions such as rainfall events and riverine inflows (Laborde et al 2010; Wang et al 2011; Zhou et al 2015; Zhang et al 2015b). The present study demonstrated that river discharge strongly influences the thermocline depth in the transitional zone. The higher discharge in May and August trips in riverine zone (Table 1) corresponded to the shallower thermocline in transitional zone during those samplings. The trend is more apparent at station 4 than that at station 3 where the water column is cold from the surface to the bottom. Similarly, Fukushima et al (2017) attributed the decrease of water temperature in Cirata Reservoir to the amount of water inflow and its temperature that affected the heat budget in the reservoir. Zhou et al (2015) demonstrated that thickness of undercurrent that flowed into reservoir is highly associated with rainfall density. The large amount of undercurrent mixed with the reservoir water and thus damaged the stratification structure of the reservoir. On the other hand, the thermocline in the lacustrine zone started at a depth of less than 1 m to 7 m, separating the epilimnion (28.6°C to 29.7°C) and the hypolimnion (≈23.2°C). In May, August, and November trips, station 7 that has the lowest surface water temperature also has a deeper thermocline layer than those at stations 5 and 6. The higher water density when surface water is cooled rendering the convectional mixing and thermocline deepening (Santos et al 2015).

Surface water in riverine and transitional zones was well-oxygenated throughout the year. The highest DO content was observed at riverine zone (≈8.9 mg/L), followed by transitional zone (≈7.6 mg/L), and lacustrine zone (≈6.5 mg/L). At the riverine zone, the DO content increased with increasing discharge as the water was re-aerated following rainfall events. This is supported by the high and significant correlation of DO with discharge ($r=0.917$, $P<0.05$). Figure 2 illustrates that the oxygenated riverine inflows greatly influenced the DO depth profile in the transitional zone whereby the DO value increased with depth and then maintained at a DO value of more than 8 mg/L at the bottom water column. Although the DO value at station 3 initially decreased with depth, it increased with depth when the riverine inflow intruded at around 5 m depth. On the other hand, the DO value quickly decreased with depth in the lacustrine zone. The depth of water column that contained healthy DO value of more than 5 mg/L for healthy life of aquatic organisms (CCME 1999; Best et al 2007) at the lacustrine zone ranged from less than 1 m to 5 m. Both the lower and upper values of this range are lower compared to the healthy DO water column of 3 m to 6 m obtained from the new large tropical Bakun Reservoir (Ling et al 2017). The DO value reached a minimum at around 6–7 m at station 5. Below the minimum, the DO value began to have a small increase again with depth at around 35 m in February and May trips. The small increase is most likely related to water circulation in the reservoir where the plumes can propagate to the deeper part of the reservoir. On the other hand, the riverine inflows intruded at around 10 m at station 6 in August and November trips rendering the DO value a minimum at the deeper water column of around 20 m compared to other months. The depth reached by the density current varies during the course of the year since water quality and density of reservoir and river change temporally. The present study demonstrates that the density currents induced by the riverine inflows can intrude and propagate down to the deeper part of the lacustrine zone at stations 5 and 6. Similarly, Elci (2008) demonstrated an increase in the

DO concentration below the thermocline in the Tahtali Reservoir, Turkey in August. The author attributed it to convective circulation introduced by lateral flow from side arms of the lake.

Unlike the water temperature and DO, surface water pH in the riverine zone varied during the course of the year, ranging from 5.1 to 6.5 and 6.2 to 7.3 at station 1 and station 2, respectively (Figure 3).

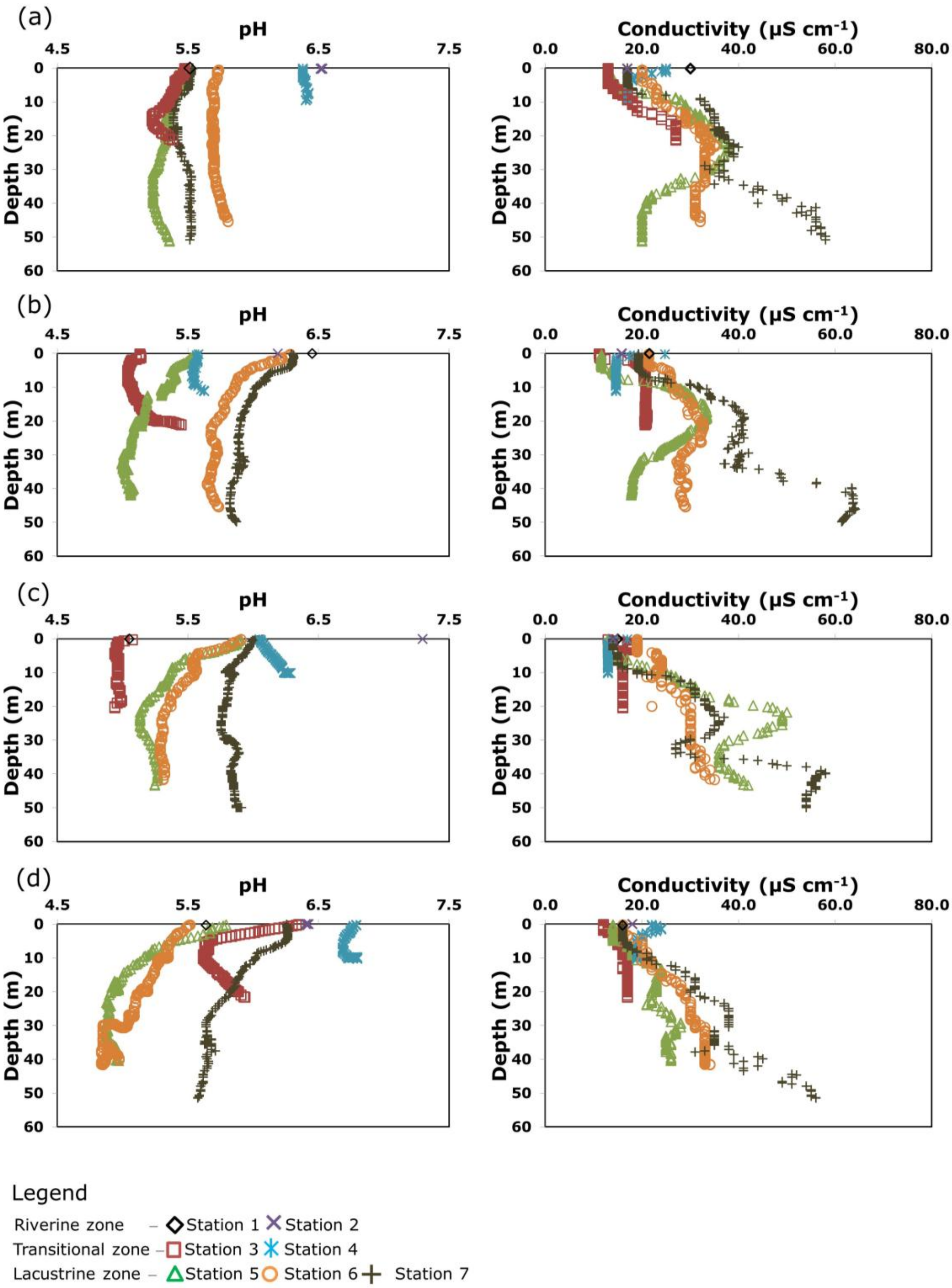

Figure 3. Depth profiles of pH and conductivity measured in (a) February, (b) May, (c) August, and (d) November 2017 at the Murum reservoir.

The water pH at station 1 located at the Plieran River was generally more acidic than at station 2 at the Danum River where it falls into Class III of the National Water Quality

Standards for Malaysia (NWQS) at all trips except May 2017 whereas at station 2, the values fall in either Class I or II. Acidification of river water at the Plieran River is most likely due to the active logging, plantation and subsistence farming at the area (Sapis et al 2018). Similarly, station 3 that received inflow from the Plieran River was more acidic than station 4 which received inflow from the Danum River, with surface water pH ranging from 5.1 to 6.3 and 5.6 to 6.8 at station 3 and station 4, respectively. The surface water pH was lower in May and August trips than in February and November trips. The low pH value in May and August trips corresponded with high turbidity value during those months indicating the organic matter brought to the area leading to reduced water pH value (Ensign & Mallin 2001). The pH depth profile of transitional zone of the reservoir was likely influenced by the inflows via dilution. In November, the riverine inflow from station 1 penetrated into station 3 as plunging intrusions, rendering the rapid decrease in pH value at station 3 from 6.4 to 5.6 which was close to the pH value from its inflow (Figure 3). On the other hand, the pH value at station 4 in August trip increased right away with depth due to the high water pH value of its inflows at station 2. In addition, the riverine inflow could sometimes influence the pH value of the whole water column in the transitional zone as demonstrated by station 4 in February and station 3 in August whereby the pH values were consistent throughout the water column and close to the pH value of the riverine inflow. The effect could also extend to the lacustrine zone as shown by the uniform pH depth profile of station 6 in the lacustrine zone in February. Nevertheless, pH value in the lacustrine zone is mostly decreasing with depth which is associated with the accumulation of CO_2 due to the low photosynthesis rate and high decomposition rate of organic matter in the deeper layers of the water column (Elci 2008). This is supported by the significant negative correlation between pH and CO_2 (r=-0.321, P<0.05). Surface CO_2 ranged from 2.0 to 9.33 mg L^{-1} whereas from 10 m depth onwards, the values ranged from 2.0 to 48.0 mg L^{-1} (Table 2).

Table 2

Free carbon dioxide (CO_2) at the sampling stations in the Murum reservoir in 2017

St	*Depth (m)*	*CO_2 (mg L^{-1})*			
		February	*May*	*August*	*November*
1	0	$6.00\pm1.00^{a,b,1}$	$5.67\pm0.58^{a,b,1}$	$9.33\pm0.58^{a,b,2}$	$6.00\pm0.00^{a,b,1}$
2	0	$3.33\pm0.58^{a,c,d,1}$	$5.67\pm0.58^{a,b,2}$	$4.33\pm0.58^{c,d,e,1}$	$2.00\pm0.00^{c,3}$
3	0	$2.00\pm0.00^{c,d}$	3.00 ± 0.00^{c}	$7.00\pm0.00^{a,b,c,d,f}$	2.00 ± 0.00^{c}
	10	$4.67\pm0.58^{a,c,1}$	$5.67\pm0.58^{a,b,1}$	$8.33\pm0.58^{a,b,f,2}$	$6.00\pm1.00^{a,b,1}$
	20	$6.67\pm0.58^{a,b,1}$	$6.33\pm0.58^{a,d,1}$	$10.67\pm1.15^{a,2}$	$6.00\pm1.00^{a,b,1}$
4	0	$2.00\pm0.00^{c,d,1}$	$4.00\pm0.00^{b,c,2}$	$3.67\pm0.58^{c,e,2}$	$2.00\pm0.00^{c,1}$
	10	1.00 ± 0.00^{d}	$4.00\pm0.00^{b,c}$	2.00 ± 0.00^{e}	$4.00\pm0.00^{a,b,c}$
5	0	$3.67\pm0.58^{a,c,d,1,2}$	$3.00\pm0.00^{c,1,3}$	$5.00\pm1.00^{c,d,e,f,2}$	$2.00\pm0.00^{c,3}$
	10	$22.33\pm0.58^{e,1}$	$14.67\pm1.15^{e,2}$	$15.67\pm1.53^{g,2}$	$16.67\pm1.61^{d,2}$
	20	$30.33\pm1.15^{f,1}$	$10.33\pm0.58^{f,2}$	$36.33\pm1.15^{h,3}$	$15.33\pm0.58^{d,4}$
	30	$24.00\pm2.00^{e,g,1}$	$15.00\pm1.00^{e,2}$	$48.00\pm2.00^{i,3}$	$21.83\pm0.76^{e,1}$
	40	$13.33\pm1.53^{h,i,1}$	$16.00\pm0.00^{e,1}$	$44.00\pm3.61^{j,2}$	$22.00\pm1.00^{e,3}$
6	0	$3.67\pm0.58^{a,c,d,1}$	$3.00\pm0.00^{c,1,2}$	$5.67\pm0.58^{b,c,d,e,f,3}$	$2.00\pm0.00^{c,2}$
	10	$6.67\pm0.58^{a,b,1,2}$	$5.50\pm0.50^{a,b,1}$	$8.00\pm1.00^{a,b,d,f,2}$	$7.00\pm0.00^{a,f,1,2}$
	20	$10.67\pm0.58^{h,j,1}$	$10.67\pm0.58^{f,1}$	$16.00\pm0.00^{g,k,2}$	$16.00\pm0.00^{d,2}$
	30	$12.00\pm1.00^{h,i,1}$	$9.00\pm1.00^{f,g,2}$	$6.00\pm1.00^{b,c,d,f,3}$	$10.00\pm0.00^{f,1,2}$
	40	$14.67\pm0.58^{i,1}$	$8.00\pm1.00^{d,g,2}$	$15.03\pm0.95^{g,1}$	$17.00\pm0.00^{d,3}$
7	0	$3.67\pm0.58^{a,c,d,1}$	$3.00\pm0.00^{c,1}$	$2.00\pm0.00^{e,2}$	$3.00\pm0.00^{b,c,1}$
	10	$8.50\pm0.50^{b,j,1}$	$16.00\pm0.00^{e,2}$	$10.67\pm1.15^{a,3}$	$16.33\pm0.58^{d,2}$
	20	$28.67\pm0.58^{f,k,1}$	$23.00\pm1.00^{h,2}$	$15.00\pm0.00^{g,3}$	$27.00\pm1.00^{g,1}$
	30	$26.33\pm1.53^{g,k,1}$	$19.67\pm0.58^{i,2}$	$19.67\pm0.58^{k,2}$	$31.00\pm1.00^{h,3}$
	40	$35.00\pm3.46^{l,1}$	$39.33\pm0.58^{b,c,1}$	$24.00\pm2.65^{l,2}$	$34.00\pm1.73^{h,1}$
	50	$41.00\pm0.00^{m,1}$	$41.67\pm0.58^{k,1}$	$24.67\pm0.58^{l,2}$	$43.67\pm3.21^{i,1}$

Means in the same column and row with the same superscript are not significantly different among stations/depths and among months respectively (p>0.05).

At station 7 of lacustrine zone, there was a consistent increasing CO_2 trend when depth increased. At other transitional and lacustrine stations, the trend of CO_2 was not that consistent due to river intrusion and circulation. However, during low river discharge of February, station 6 experienced the same trend as station 7. CO_2 in turn is significantly and positively correlated with BOD_5 ($r=0.500$, $P<0.05$). In general, BOD_5 increases with depth and it is especially evident with station 7 of lacustrine zone (Table 3).

Table 3

Biochemical oxygen demand (BOD_5) at the sampling stations in the Murum reservoir in 2017

St	Depth (m)	BOD_5 (mg L^{-1})			
		February	May	August	November
1	0	$3.24\pm0.10^{a,1}$	$3.21\pm0.09^{a,1}$	$3.62\pm0.03^{a,2}$	$3.40\pm0.11^{a,b,1,2}$
2	0	$3.31\pm0.10^{a,1}$	$4.51\pm0.07^{b,2}$	$1.95\pm0.08^{b,c,d,3}$	$2.56\pm0.07^{c,d,e,4}$
3	0	$2.13\pm0.07^{b,c,1}$	$1.79\pm0.34^{c,d,e,1,2}$	$0.89\pm0.11^{e,f,3}$	$1.46\pm0.07^{f,g,h,2}$
	10	$0.49\pm0.13^{d,1}$	$0.78\pm0.12^{f,g,1}$	$2.98\pm0.19^{g,2}$	$2.00\pm0.06^{c,f,i,3}$
	20	$0.70\pm0.05^{d,e,f,1}$	$0.58\pm0.11^{f,1}$	$3.62\pm0.55^{a,2}$	$2.32\pm0.39^{c,d,e,i,3}$
4	0	$1.57\pm0.01^{g,1}$	$2.18\pm0.17^{c,h,2}$	$1.83\pm0.19^{b,c,d,h,1,2}$	$1.41\pm0.21^{f,g,h,1}$
	10	$0.65\pm0.08^{d,e,1}$	$3.08\pm0.06^{a,2}$	$1.64\pm0.07^{b,h,3}$	$2.54\pm0.13^{c,d,e.4}$
5	0	$2.02\pm0.12^{b,c,1}$	$1.67\pm0.39^{d,e,i,1}$	$0.77\pm0.04^{e,2}$	$1.96\pm0.32^{c,f,i,1}$
	10	$0.61\pm0.13^{d,e,1}$	$2.07\pm0.06^{c,d,h,2}$	$1.38\pm0.12^{f,h,i,3}$	$2.80\pm0.34^{a,d,e,4}$
	20	$1.02\pm0.19^{f,h,i,1}$	$4.20\pm0.31^{b,2}$	$3.13\pm0.20^{a,g,3}$	$3.81\pm0.57^{b,2,3}$
	30	$2.24\pm0.02^{b,c,1}$	$1.60\pm0.07^{d,e,i,2}$	$5.80\pm0.15^{j,3}$	$3.73\pm0.14^{b,4}$
	40	$0.90\pm0.03^{e,f,h,1}$	$2.30\pm0.08^{h,2}$	$3.30\pm0.08^{a,g,3}$	$3.68\pm0.64^{b,3}$
6	0	$2.01\pm0.09^{b,1}$	$1.20\pm0.10^{g,i,2}$	$1.67\pm0.11^{b,h,3}$	$1.26\pm0.14^{f,g,h,j,2}$
	10	$0.56\pm0.06^{d,1}$	$1.39\pm0.04^{i,2}$	$1.51\pm0.07^{b,h,i,2}$	$0.72\pm0.04^{g,j,3}$
	20	$1.09\pm0.02^{h,i,1}$	$1.97\pm0.06^{c,d,h,2}$	$1.72\pm0.08^{b,c,h,2}$	$4.88\pm0.30^{k,3}$
	30	$1.13\pm0.03^{h,i,j,1}$	$2.19\pm0.13^{c,h,2}$	$2.23\pm0.09^{c,d,2}$	$0.49\pm0.08^{j,3}$
	40	$0.49\pm0.01^{d,1}$	$2.16\pm0.14^{c,h,2}$	$2.30\pm0.10^{d,2}$	$1.15\pm0.10^{g,h,j,3}$
7	0	$1.42\pm0.04^{g,j,1}$	$1.19\pm0.09^{g,i,2}$	$1.03\pm0.04^{e,f,i,2}$	$2.05\pm0.08^{c,d,f,i,3}$
	10	$1.11\pm0.09^{h,i,j,1}$	$1.88\pm0.08^{c,d,2}$	$2.88\pm0.01^{g,3}$	$1.74\pm0.10^{f,h,i,2}$
	20	$4.40\pm0.11^{k,1}$	$3.18\pm0.13^{a,2}$	$1.50\pm0.10^{b,h,i,3}$	$2.44\pm0.15^{c,d,e,i,4}$
	30	$2.34\pm0.09^{c,1}$	$3.06\pm0.09^{a,2}$	$1.38\pm0.07^{f,h,i,3}$	$3.07\pm0.14^{a,b,e,2}$
	40	$1.25\pm0.08^{g,i,j,1}$	$5.96\pm0.06^{j,2}$	$1.71\pm0.05^{b,h,3}$	$2.57\pm0.20^{c,d,e,4}$
	50	$2.14\pm0.02^{b,c,1}$	$6.49\pm0.03^{k,2}$	$3.52\pm0.12^{a,3}$	$4.75\pm0.21^{k,4}$

Means in the same column and row with the same superscript are not significantly different among stations/depths and among months respectively ($p>0.05$).

Similar to the trend of CO_2, there were times when the maximum BOD_5 was not at the deepest water column due to similar reason. At the riverine zone, BOD_5 at station 1 consistently fall into Class III of NWQS due to organic pollutants from logging and oil palm plantation activities upstream. At station 2, BOD_5 also fall in Class III twice out of four times with the remainder complying with Class II. At transitional and lacustrine zones, BOD_5 occasionally fall in Class III at depth of 10 m or more.

Surface conductivity in the riverine zone of the Murum reservoir was low, with an average of 20.6 μS/cm and 16.2 μS/cm at stations 1 and 2, respectively. Conductivity at the riverine zone was affected by temperature as increasing mobility of ions occurs when temperature increases. This is supported by the high and significant correlation between temperature and conductivity ($r=0.720$, $P<0.05$). Similar to water pH, vertical distribution of conductivity in the transitional zone was influenced mainly by the conductivity of its inflow. Conductivity value in the transitional zone was consistent throughout the water column where it was close to the conductivity of riverine inflows (Figure 3). On the other hand, conductivity value tends to increase with depth when riverine inflow has high conductivity whereas conductivity value decrease with depth if riverine inflow was low in conductivity. Figure 3 illustrates that conductivity value in the lacustrine zone increased with depth but was interrupted at the deeper water column.

Decomposition of organic matter in the deeper water column increased the ion concentration, thus increasing the electrical conductivity (Elci 2008). This is supported by the significant correlation between conductivity and BOD_5 (r=0.375, P<0.05) where BOD_5 (Table 3) is a measure of organic matter content. The interruption at the deeper water column was most probably attributed to the dilution effects by density currents induced by the riverine inflows which propagated down to the deeper part of the lacustrine zone. Similarly, higher electrical conductivity at most of the stations in the new Bakun reservoir at 30 m depth was observed (Ling et al 2016). Zhang et al (2015a) demonstrated that conductivity levels in the bottom water of irrigation reservoirs in Virginia and Maryland were equal to or higher than those at the surface. The authors suggested that the electrical conductivity variation are associated with thermal stratification as the top-bottom conductivity differences were minimal during the non-stratification period and enhanced during the stratification period.

The riverine zone of the Murum Reservoir is extremely turbid compared to the transitional and lacustrine zones as the turbidity consistently exceeded the Class II limit (50 NTU) according to NWQS. In addition, the TSS at riverine zone consistently fall in Class V (300 mg L^{-1}) of NWQS. Between the two stations in the riverine zone, turbidity and TSS at station 1 were relatively consistent throughout the year, ranging from 453.5 NTU to 619.6 NTU (Figure 4) and 533.7 mg L^{-1} to 701.5 mg L^{-1} (Table 4) respectively whereas a peak turbid condition, 1217.0 NTU and 2,646.5 mg L^{-1} was observed at station 2. The turbidity values at the riverine zone are confirmed by the ex-situ TSS values with a very high correlation (r=0.954, P<0.05) indicating the organic and inorganic particles of erosion from cleared forest and logging road. The turbid condition was highly associated with the increasing river velocity due to rainfall event (Zhou et al 2015). The present turbidity value is substantially higher than the turbidity of inflow into the Bakun reservoir in the same region (Ling et al 2015). The lowest surface turbidity was found in the lacustrine zone where it was mostly undetectable throughout the year. Vertical profiling shows that turbidity and TSS in lacustrine zone increased with depth. The higher turbidity and TSS at the bottom was consistent with literature where it was mostly attributed to the settling of particulate matter (Zhang et al 2015a; Ling et al 2016, 2017). The surface turbidity and TSS of the transitional zone fluctuated throughout the year. Station 4 also showed high turbidity and TSS due to soil disturbance as a result active logging activities and oil palm plantation development. In addition, there was rainfall event prior to sampling at all the trips except February 2017. High rate of soil loss from oil palm development activities has been shown in a simulated rainfall study with fully and half bare soil (Sahat et al 2016). The vertical distribution of turbidity in the transitional zone also varied throughout the year as illustrated in Figure 4. In the February trip, turbidity steadily increased with depth until it was close to the turbidity of the inflow. The upstream river with high turbidity value intruded into the transitional zone where the maximum turbidity was observed. Turbidity at station 3 reached its maximum at the bottom of the water column whereas at station 4 it reached its maximum at a depth of 4 m and remained constant at the deeper water column. TSS at station 3 was consistently high at 10 m and 20 m depths with the 20 m depth showing higher values than 10 m depth most of the time. The depth reached by the density current varied between stations in the transitional zone due to the variation in sediment-laden inflow water. If the amount of the sediment-laden inflow water is high, it could affect the whole water column of transitional zone as occurred in May and August where the whole water column of stations 3 and 4 was high in turbidity. In addition, the turbidity values and TSS at station 4 further increased with depth during both of those trips. A decrease in turbidity value and TSS at station 4 was only observed in November trip due to the lowest discharge at station 2. On the other hand, turbidity at station 3 was consistent throughout the water column in the May trip while a relatively lower turbidity was observed at a depth of less than 1 m at station 3 in August. In the lacustrine zone, maximum TSS occurred at either 40 m or 50 m depth as solids move downwards when water becomes stagnant. This was also observed in Bakun Reservoir below the Murum Dam (Ling et al 2017).

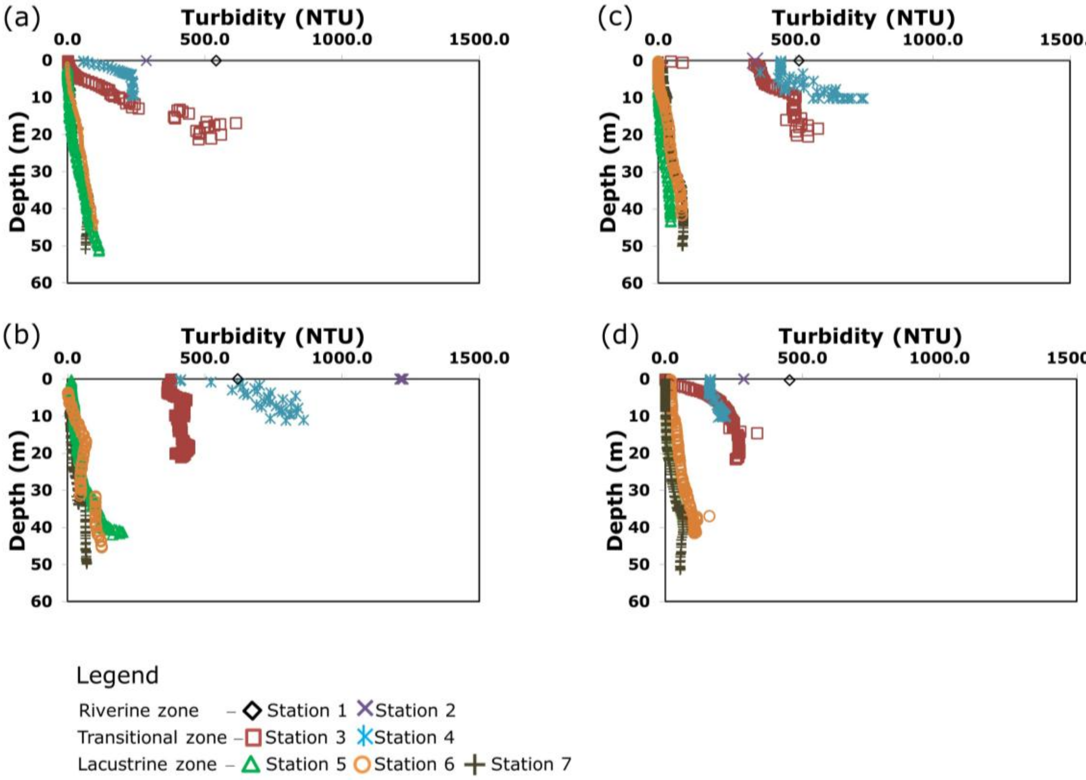

Figure 4. Depth profiles of turbidity measured in (a) February, (b) May, (c) August, and (d) November 2017 at the Murum reservoir.

Table 4

Total suspended solids (TSS) at the sampling stations in the Murum reservoir in 2017

St	*Depth (m)*	*TSS (mg L^{-1})*			
		February	*May*	*August*	*November*
1	0	540.00±25.00^{a,1,2}	533.75±54.75^{a,1}	663.20±41.90^{a,1,2}	701.50±144.96^{a,2}
2	0	370.00±10.00^{b,1}	2646.50±143.00^{b,2}	433.50±2.50^{b,1}	304.00±3.67^{b,1}
3	0	5.00±1.00^{c,1,2}	2.80±0.80^{c,1}	20.33±3.48^{c,3}	8.89±1.64^{c,2}
	10	435.00±8.66^{d,1}	339.83±16.93^{d,1,2}	732.07±98.01^{a,d,3}	207.56±35.81^{d,2}
	20	211.67±12.58^{e,1}	486.00±31.63^{a,2}	746.50±34.45^{d,3}	345.33±39.88^{b,4}
4	0	17.33±3.06^{c,f,1}	6.42±0.69^{c,2}	14.22±2.78^{c,1}	5.60±0.80^{c,2}
	10	243.33±5.77^{g,1}	736.89±63.46^{e,2}	461.70±30.70^{b,3}	100.87±7.58^{e,4}
5	0	24.00±2.00^{c,f,h,i,1}	5.90±0.70^{c,2}	4.11±0.51^{c,2}	3.87±0.66^{c,2}
	10	8.75±1.25^{c,f,1}	18.00±0.50^{c,2}	10.73±0.64^{c,1}	8.86±1.00^{c,1}
	20	18.00±2.00^{c,f,h,1}	24.00±1.00^{c,2}	15.07±0.46^{c,1,3}	12.75±2.02^{c,3}
	30	40.00±5.00^{h,i,j,k,1}	23.50±2.78^{c,2}	58.75±6.25^{c,3}	43.33±1.51^{c,e,1}
	40	48.33±2.89^{k,j,l,1,2}	37.83±6.64^{c,1}	23.00±0.00^{c,3}	60.07±6.35^{c,e,2}
6	0	8.75±1.25^{c,f,1}	2.56±0.31^{c,2}	8.30±0.70^{c,1}	5.39±0.87^{c,3}
	10	9.00±1.00^{c,f,1}	9.38±1.65^{c,1}	9.29±0.43^{c,1}	7.05±1.26^{c,1}
	20	40.00±0.00^{h,i,j,k,1}	60.07±4.11^{c,2}	38.48±2.88^{c,1}	21.73±1.03^{c,3}
	30	45.00±0.00^{i,j,k,l,1}	40.67±5.69^{c,1}	53.41±0.19^{c,2}	30.78±2.39^{c,e,3}
	40	58.33±7.64^{j,l,1}	65.47±8.35^{c,1}	74.58±3.82^{c,1}	71.08±5.08^{c,e,1}
7	0	5.24±0.82^{c,1,2}	3.75±0.63^{c,1}	7.50±2.05^{c,2}	4.07±0.68^{c,1}
	10	15.00±1.00^{c,f,1}	16.47±0.64^{c,1}	12.00±1.71^{c,2}	6.89±0.44^{c,3}
	20	11.00±1.00^{c,f,1}	20.00±1.31^{c,2}	24.33±3.06^{c,2}	13.59±0.75^{c,1}
	30	30.67±1.15^{f,h,i,k,1}	17.93±1.21^{c,2}	42.72±2.90^{c,3}	30.65±3.65^{c,e,1}
	40	65.00±5.00^{l,1,2}	51.08±1.51^{c,3}	74.86±6.15^{c,1}	58.24±4.66^{c,e,2,3}
	50	62.50±6.61^{l,1,2}	62.92±2.24^{c,1,2}	71.86±9.56^{c,1}	53.53±4.62^{c,e,2}

Means in the same column and row with the same superscript are not significantly different among stations/depths and among months respectively ($p>0.05$).

COD at the surface water of the riverine zone was high, within station 1 and station 2 ranging from 46.00 to 69.33 mg L^{-1} and 28.00-120.00 mg L^{-1} respectively (Table 5) and they fall in Class III/IV/V of NWQS. The high COD water flowed to the transitional zone, influencing the COD there. For instance, in May, the highest value of 120 mg L^{-1} at station 2 showed up the highest at 10 m depth of station 4 with a diluted value of 60.00 mg L^{-1}. Similarly, the highest value at station 1 in February affected the COD of station 3 with a surface COD of 52.0 mg L^{-1} and a decreasing trend as depth increases at that station. COD is significantly correlated with turbidity and TSS (r=0.630 and 0.725 respectively, $P<0.05$) whereas the correlation between BOD_5 with TSS were significant but weak (r=0.237, 0.257, $P<0.05$). In addition, COD values were far larger than BOD_5 values. These observations indicate the dominance of organic material which is resistant to biodegradation by ordinary micrororganisms in the water originating from upstream logging and road construction activities (Woodard & Curran Inc. 2006). In the transitional and lacustrine zone, the submerged living things such as logs are degrading resulting in higher COD as depth increased. TAN in the lacustrine zone increased with depth (Table 6) as ammonia accumulated in the deeper water column where oxygen is lacking for its oxidation. This is supported by the significant negative correlation with DO (r=-0.437, $P<0.05$). The source of TAN is the organic matter in the reservoir especially in the deeper region. This is evidenced by the significant correlation between TAN with BOD_5 (r=0.334, $P<0.05$). TAN values mostly complied with Class II of NWQS (0.30 mg L^{-1}) except for occasional violations especially in the deeper water column. For the water at the surface, station 3 was the only station which falls in Class III in May. TAN contributed to the conductivity as supported by the high and significant correlation (r=0.753, $P<0.05$). In addition, TAN accumulation is similar to CO_2 supported by significant correlation (r=0.743, $P<0.05$).

Table 5

Chemical oxygen demand (COD) at the sampling stations in the Murum reservoir in 2017

St	*Depth (m)*	*COD (mg L^{-1})*			
		February	*May*	*August*	*November*
1	0	69.33±12.22^{a,1}	69.33±4.62^{a,1}	57.60±3.84^{a,1,2}	46.00±5.52^{a,2}
2	0	28.00±4.00^{b,c,d,e,f,1}	120.00±16.00^{b,2}	30.72±0.00^{b,c,1}	29.44±0.00^{b,1}
3	0	52.00±4.00g^{g,h,1}	32.00±8.00^{c,d,2}	7.68±0.00^{d,3}	11.04±0.00^{c,d,3}
	10	48.00±8.00^{g,h,i,1,2}	53.33±9.24^{a,e,1}	33.28±4.43^{b,c,2,3}	23.31±2.12^{e,3}
	20	40.00±8.00^{c,d,g,h,i,1,2}	53.33±9.24^{a,e,1}	30.72±0.00^{b,c,2,3}	23.31±2.12^{e,3}
4	0	12.00±4.00^{b,j,1}	8.00±0.00^{f,1}	34.56±3.84^{b,2}	12.88±1.84^{c,d,1}
	10	48.00±0.00^{g,h,i,1}	60.00±4.00^{a,2}	35.84±4.43^{b,3}	15.95±4.25^{c,4}
5	0	40.00±0.00^{c,d,g,h,i,1}	8.00±0.00^{f,2}	25.60±4.43^{b,c,e,3}	7.36±0.00^{d,f,2}
	10	36.00±4.00^{c,d,e,g,i,1}	36.00±4.00^{c,e,1}	15.36±0.00^{d,e,2}	7.36±0.00^{d,f,3}
	20	32.00±0.00^{c,d,e,f,i,1}	36.00±4.00^{c,e,1,2}	26.88±3.84^{b,c,2}	12.88±1.84^{c,d,3}
	30	28.00±4.00^{b,c,d,e,f,1}	24.00±0.00^{c,d,f,g,1}	15.36±0.00^{d,e,2}	7.36±0.00^{d,f,3}
	40	44.00±4.00^{c,g,h,i,1}	16.00±8.00^{d,f,g,2,3}	28.16±4.43^{b,c,2}	7.36±0.00^{d,f,3}
6	0	20.00±4.00^{b,e,f,j,1,2}	16.00±0.00^{d,f,g,1}	25.60±4.43^{b,c,e,2}	12.88±1.84^{c,d,1}
	10	29.33±4.62^{c,d,e,f,1}	20.00±4.00^{c,d,f,g,1,2}	11.52±3.84^{d,2,3}	3.68±0.00^{f,3}
	20	37.33±4.62^{c,d,g,i,1}	16.00±0.00^{d,f,g,2}	23.04±0.00^{c,e,3}	7.36±0.00^{d,f,4}
	30	26.67±4.62^{b,d,e,f,1}	36.00±4.00^{c,e,1}	26.88±3.84^{b,c,1}	7.36±0.00^{d,f,2}
	40	8.00±0.00^{j,1}	8.00±0.00^{f,1}	26.88±3.84^{b,c,2}	7.36±0.00^{d,f,1}
7	0	16.00±0.00^{b,f,j}	8.00±0.00^{f}	15.36±0.00^{d,e}	7.36±0.00^{d,f}
	10	20.00±4.00^{b,e,f,j,1}	12.00±4.00^{f,g,1,2}	11.52±3.84^{d,1,2}	7.36±0.00^{d,f,2}
	20	28.00±4.00^{b,c,d,e,f,1}	28.00±4.00^{c,d,g,1}	34.56±3.84^{b,1}	3.68±0.00^{f,2}
	30	40.00±8.00^{c,d,g,h,i,1}	20.00±4.00^{c,d,f,g,2}	15.36±0.00^{d,e,2,3}	7.36±0.00^{d,f,3}
	40	56.00±0.00^{a,h,1}	12.00±4.00^{f,g,2}	26.88±3.84^{b,c,3}	45.39±2.12^{a,4}
	50	24.00±8.00^{b,d,e,f,j,1,2}	12.00±4.00^{f,g,1}	35.84±4.43^{b,2}	13.49±2.12^{c,1}

Means in the same column and row with the same superscript are not significantly different among stations/depths and among months respectively ($p>0.05$).

Table 6
Total ammonia nitrogen (TAN) at the sampling stations in the Murum reservoir in 2017

St	Depth (m)	TAN (mg L^{-1})			
		February	*May*	*August*	*November*
1	0	$0.17\pm0.00^{a,1}$	$0.29\pm0.01^{a,b,2}$	$0.08\pm0.01^{a,b,c,d,3}$	$0.13\pm0.02^{a,4}$
2	0	$0.04\pm0.01^{b,1}$	$0.11\pm0.02^{c,d,e,2}$	$0.17\pm0.03^{e,f,g,3}$	$0.05\pm0.00^{b,c,d,1}$
3	0	$0.05\pm0.00^{b,1}$	$0.33\pm0.00^{a,f,2}$	$0.21\pm0.01^{e,f,h,3}$	$0.04\pm0.00^{b,c,1}$
	10	$0.08\pm0.01^{b,c,1}$	$0.36\pm0.02^{f,g,2}$	$0.16\pm0.02^{e,f,g,i,3}$	$0.09\pm0.01^{e,f,1}$
	20	$0.12\pm0.01^{d,e,1}$	$0.26\pm0.02^{b,h,2}$	$0.16\pm0.00^{e,g,i,3}$	$0.06\pm0.00^{b,d,e,4}$
4	0	$0.06\pm0.01^{b,c,1}$	$0.07\pm0.01^{c,d,i,1}$	$0.24\pm0.02^{h,2}$	$0.05\pm0.00^{b,c,d,1}$
	10	$0.23\pm0.01^{f,1}$	$0.06\pm0.01^{c,i,2}$	$0.16\pm0.02^{e,g,i,3}$	$0.06\pm0.01^{b,d,2}$
5	0	$0.04\pm0.00^{b,1}$	$0.26\pm0.01^{b,h,2}$	$0.22\pm0.01^{f,h,3}$	$0.03\pm0.00^{c,1}$
	10	$0.32\pm0.01^{g,1}$	$0.46\pm0.01^{j,2}$	$0.16\pm0.03^{e,g,i,3}$	$0.05\pm0.00^{b,c,d,4}$
	20	$0.52\pm0.03^{h,1}$	$0.53\pm0.01^{k,1}$	$0.40\pm0.02^{j,2}$	$0.13\pm0.00^{a,3}$
	30	$0.33\pm0.01^{g,1,2}$	$0.36\pm0.01^{f,g,1}$	$0.55\pm0.04^{k,3}$	$0.27\pm0.01^{g,h,2}$
	40	$0.09\pm0.01^{c,d,1}$	$0.25\pm0.02^{b,h,2}$	$0.09\pm0.02^{a,b,c,1}$	$0.26\pm0.01^{g,2}$
6	0	$0.04\pm0.01^{b,1}$	$0.06\pm0.01^{c,i,1,2}$	$0.06\pm0.00^{a,b,d,2}$	$0.06\pm0.01^{b,d,e,1,2}$
	10	$0.05\pm0.01^{b,c,1}$	$0.10\pm0.02^{c,d,e,2}$	$0.13\pm0.01^{c,g,i,3}$	$0.11\pm0.01^{a,f,2,3}$
	20	$0.14\pm0.01^{a,e,1,2}$	$0.18\pm0.03^{m,l,1}$	$0.26\pm0.02^{h,3}$	$0.11\pm0.01^{a,f,2}$
	30	$0.22\pm0.01^{f,1}$	$0.19\pm0.02^{l,2}$	$0.11\pm0.01^{a,c,i,3}$	$0.16\pm0.00^{i,2}$
	40	$0.17\pm0.01^{a,1}$	$0.12\pm0.02^{d,e,2}$	$0.03\pm0.01^{d,3}$	$0.31\pm0.02^{j,4}$
7	0	$0.04\pm0.01^{b,1}$	$0.13\pm0.02^{e,m,2}$	$0.04\pm0.00^{b,d,1}$	$0.05\pm0.01^{b,c,d,1}$
	10	$0.05\pm0.00^{a,1}$	$0.05\pm0.01^{i,1}$	$0.06\pm0.00^{a,b,d,1,2}$	$0.07\pm0.01^{d,e,2}$
	20	$0.38\pm0.01^{i,1}$	$0.22\pm0.01^{h,l,2}$	$0.32\pm0.01^{l,3}$	$0.30\pm0.01^{h,j,3}$
	30	$0.41\pm0.01^{i,1}$	$0.40\pm0.01^{g,1,2}$	$0.38\pm0.02^{l,j,2}$	$0.56\pm0.01^{k,3}$
	40	$0.86\pm0.02^{j,1}$	$0.54\pm0.03^{k,2}$	$0.57\pm0.01^{k,2}$	$0.35\pm0.02^{l,3}$
	50	$0.91\pm0.02^{k,1}$	$0.85\pm0.01^{n,2}$	$0.67\pm0.02^{m,3}$	$0.64\pm0.01^{m,3}$

Means in the same column and row with the same superscript are not significantly different among stations/depths and among months respectively ($p>0.05$).

Conclusions. The present study demonstrated the spatio-temporal profiles of water quality at the three different zones in the Murum reservoir in Sarawak. Water quality parameters in the transitional and lacustrine zones exhibited spatiotemporal variations in vertical distribution. The riverine inflows were well-oxygenated but in acidic and turbid conditions due to organic materials from the river basin. Intrusion of the colder sediment-laden inflows from the riverine zone influenced the depth profiles of the transitional and lacustrine zones in the reservoir. The impact is even more apparent particularly after rainfall events with high volume of riverine inflows into the reservoir. At the lacustrine zone, though turbidity reduced drastically to comply with Class II for at least 20 m depth, the column of dissolved oxygen for healthy aquatic organisms is still shallow and most of the time it is too acidic and thus not suitable for aquaculture yet. Thus, there is an urgent need to reduce the input of solids and organic matter into the reservoir for the management of fisheries and considerations for aquaculture industry in the future.

Acknowledgements. The authors appreciate the financial support provided by Sarawak Energy Berhad through Grant No. GL(F07)/SEB/4C/2013(26), and the facilities provided by Malaysia Sarawak University.

References

Abery N. W., Sukadi F., Budhiman A. A., Kartamihardja E. S., Koeshendrajana S., Buddhiman A. A., De Silva S. S., 2005 Fisheries and cage culture of three reservoirs in West Java, Indonesia; a case study of ambitious development and resulting interactions. Fisheries Management and Ecology 12(5):315–330.
Agostinho A. A., Pelicice F. M., Gomes L. C., 2008 Dams and the fish fauna of the Neotropical region: impacts and management related to diversity and fisheries.

Brazilian Journal of Biology 68(4):1119–1132.
Araujo F. G., de Azevedo M. C. C., Ferreira M. D. L., 2011 Seasonal changes and spatial variation in the water quality of a eutrophic tropical reservoir determined by the inflowing river. Lake and Reservoir Management 27(4):343–354.
Best M. A., Wither A. W., Coates S., 2007 Dissolved oxygen as a physico-chemical supporting element in the Water Framework Directive. Marine Pollution Bulletin 55:53–64.
Chapra S. C., 1997 Surface water-quality modeling. McGraw- Hill Inc., New York.
Costa-Pierce B., 1997 From farmers to fishers: Developing reservoir aquaculture for people displaced by dams. World Bank Technical Paper No. 369, Fisheries Series, The World Bank, Washington D.C., 72 p.
Elci S., 2008 Effects of thermal stratification and mixing on reservoir water quality. Limnology 9(2):135–142.
Ensign S. H., Mallin M. A., 2001 Stream water quality changes following timber harvest in a coastal plain swamp forest. Water Research 35(14):3381–3390.
Faithful J. W., Griffiths D. J., 2000 Turbid flow through a tropical reservoir (Lake Dalrymple, Queensland, Australia): responses to a summer storm event. Lakes & Reservoirs: Research and Management 5(4):231–247.
Fukushima T., Matsushita B., Subehi L., Setiawan F., Wibowo H., 2017 Will hypolimnetic waters become anoxic in all deep tropical lakes? Scientific Reports 7:45320; doi: 10.1038/srep45320.
Jones J. R., Knowlton M. F., Obrecht D. V., Graham J. L., 2011 Temperature and oxygen in Missouri reservoirs. Lake and Reservoir Management 27(2):173–182.
Laborde S., Antenucci J. P., Copetti D., Imberger J., 2010 Inflow intrusions at multiple scales in a large temperate lake. Limnology and Oceanography 55(3):1301–1312.
Li X., Huang T., Ma W., Sun X., Zhang H., 2015 Effects of rainfall patterns on water quality in a stratified reservoir subject to eutrophication: implications for management. Science of the Total Environment 521–522:27–36.
Ling T. Y., Gerunsin N., Soo C. L., Nyanti L., Sim S. F., Grinang J., 2017 Seasonal changes and spatial variation in water quality of a large young tropical reservoir and its downstream river. Journal of Chemistry Article ID 8153246, 16 pages, https://doi.org/10.1155/2017/8153246.
Ling T. Y., Nyanti L., John-Masion A. S., 2015 Water quality of rivers that flow into Bakun hydroelectric dam reservoir, Sarawak, Malaysia. ESTEEM Academic Journal 11 (Special Issue 1):9–16.
Ling T. Y., Nyanti L., Leong C. K., Wong K. M., 2013 Comparison of water quality at different locations at batang Ai Reservoir, Sarawak, Malaysia. World Applied Sciences Journal 26(11):1473-1481.
Ling T. Y., Nyanti L., Muan T., Grinang J., Sim S. F., Mujahid A., 2016 Physicochemical parameters of Bakun reservoir in Belaga, Sarawak, Malaysia, 13 months after reaching full supply level. Sains Malaysiana 45(2):157–166.
Ling T. Y., Tan A. C., Nyanti L., Sim S. F., Grinang J., Lee K. S. P., Ganyai T., 2018 Seasonal variations in water quality of a tropical reservoir: considerations for cage aquaculture expansion. AACL Bioflux 11(2):333-347.
Nyanti L., Ling T. Y., Grinang J., 2012 Physico-chemical characteristics in the filling phase of Bakun hydroelectric reservoir, Sarawak, Malaysia. International Journal of Applied Science and Technology 2(6):92–101.
Sahat S., Yusop Z., Askari M., Ziegler A. D., 2016 Estimation of soil erosion rates in oil palm plantation with different land cover. IOP Conference Series: Material Science & Engineering 136:012086, doi:10.1088/1757-899X/136/1/012086.
Santos R. M., Saggio A. A., Silva T. L., Negreiros N. F., Rocha O., 2015 Short-term thermal stratification and partial overturning events in a warm polymictic reservoir: effects on distribution of phytoplankton community. Brazilian Journal of Biology 75(1):19–29.
Sapis A., Noweg G. T., Nyanti L., Grinang J., 2018 Effects of land use on fish assemblages in inundated area of Pleiran river and Danum river sections of Murum reservoir, Belaga, Sarawak. Malaysian Applied Biology 47(1):223–230.

Sapis A., Nyanti L., Ling T. Y., Sim S. F., Grinang J., 2017 Assessing water quality of Murum Reservoir halfway through impoundment. Sains Malaysiana 46(12):2367–2374.
Wang S., Qian X., Han B. P., Wang Q. H., Ding Z. F., 2011 Physical limnology of a typical subtropical reservoir in south China. Lake and Reservoir Management 27(2):149–161.
Zhang H., Richardson P. A., Belayneh B. E., Ristvey A., Lea-Cox J., Copes W. E., Moorman G. W., Hong C., 2015a Characterization of water quality in stratified nursery recycling irrigation reservoirs. Agricultural Water Management 160:76–83.
Zhang Y., Wu Z., Liu M., He J., Shi K., Zhou Y., Wang M., Liu X., 2015b Dissolved oxygen stratification and response to thermal structure and long-term climate change in a large and deep subtropical reservoir (Lake Qiandaohu, China). Water Research 75:249–258.
Zhou Z. Z., Huang T. L., Ma W. X., Li Y., Zeng K., 2015 Impacts of water quality variation and rainfall runoff on Jinpen Reservoir, in Northwest China. Water Science and Engineering 8(4):301–308.
*** APHA (American Public Health Association), 2005 Standard methods for the examination of water and wastewater 21st edition. American Public Health Association, Washington, 1220 p.
*** CCME, 1999 Canadian water quality guidelines for the protection of aquatic life: dissolved oxygen (freshwater). In: Canadian Environmental Quality Guidelines, 1999, Winnipeg, Canada: Canadian Council of Ministers of the Environment 1–6.
*** HACH, 2002 Water Analysis Handbook. 4th edition, Loveland: HACH Co.
*** Woodard & Curran Inc., 2006 Industrial Waste Treatment Handbook. 2nd Edition, Elsevier Inc., 532 p.

Received: 16 May 2018. Accepted: 24 June 2019. Published online: 30 June 2019.
Authors:
Teck Yee Ling, Malaysia Sarawak University, Faculty of Resource Science and Technology, Malaysia, Sarawak, 94300 Kota Samarahan, e-mail: tyling@unimas.my
Kong Siew Phang, Malaysia Sarawak University, Faculty of Resource Science and Technology, Malaysia, Sarawak, 94300 Kota Samarahan, e-mail: kongsiew@yahoo.com
Chen Lin Soo, Malaysia Sabah University, Institute for Tropical Biology and Conservation, Malaysia, Sabah, 88400 Kota Kinabalu, e-mail: qianlin1112@gmail.com
Lee Nyanti, Malaysia Sarawak University, Faculty of Resource Science and Technology, Malaysia, Sarawak, 94300 Kota Samarahan, e-mail: nyantilee2@gmail.com
Siong Fong Sim, Malaysia Sarawak University, Faculty of Resource Science and Technology, Malaysia, Sarawak, 94300 Kota Samarahan, e-mail: sfsim@unimas.my
Jongkar Grinang, Malaysia Sarawak University, Institute of Biodiversity and Environmental Conservation, Malaysia, Sarawak, 94300 Kota Samarahan, e-mail: gjongkar@unimas.my

How to cite this article:
Ling T. C., Phang K. S., Soo C. L., Nyanti L., Sim S. F., Grinang J., 2019 Spatiotemporal profiles of water quality at a new large tropical hydroelectric dam reservoir. AACL Bioflux 12(3):893-907.